





# Phospholipase D $\alpha$ 6 and phosphatidic acid regulate gibberellin signaling in rice

Huasheng Cao<sup>1,2</sup> , Rong Gong<sup>2</sup>, Shu Yuan<sup>1</sup> , Yuan Su<sup>3,4</sup>, Weixin Lv<sup>1</sup>, Yimeng Zhou<sup>1</sup>, Qingqing Zhang<sup>1</sup>, Xianjun Deng<sup>1</sup>, Pan Tong<sup>1</sup>, Shihu Liang<sup>2,\*</sup>, Xuemin Wang<sup>3,4,\*\*</sup>  & Yueyun Hong<sup>1,\*\*\*</sup> 

## Abstract

Phospholipase D (PLD) hydrolyzes membrane lipids to produce phosphatidic acid (PA), a lipid mediator involved in various cellular and physiological processes. Here, we show that PLD $\alpha$ 6 and PA regulate the distribution of GIBBERELLIN (GA)-INSENSITIVE DWARF1 (GID1), a soluble gibberellin receptor in rice. PLD $\alpha$ 6-knockout (KO) plants display less sensitivity to GA than WT, and PA restores the mutant to a normal GA response. GA binds to GID1, as documented by liposome binding, fat immunoblotting, and surface plasmon resonance. Arginines 79 and 82 of GID1 are two key amino acid residues required for PA binding and also for GID1's nuclear localization. The loss of PLD $\alpha$ 6 impedes GA-induced nuclear localization of GID1. In addition, PLD $\alpha$ 6-KO plants attenuated GA-induced degradation of the DELLA protein SLENDER RICE1 (SLR1). These data suggest that PLD $\alpha$ 6 and PA positively mediate GA signaling in rice via PA binding to GID1 and promotion of its nuclear translocation.

**Keywords** gibberellin signaling; GID1 receptor; phosphatidic acid; Phospholipase; rice

**Subject Categories** Membranes & Trafficking; Plant Biology; Signal Transduction

**DOI** 10.15252/embr.202051871 | Received 15 October 2020 | Revised 7 June 2021 | Accepted 22 July 2021 | Published online 16 August 2021

**EMBO Reports (2021) 22: e51871**

## Introduction

Gibberellins (GAs) are important hormones affecting plant growth and development throughout the life cycle, ranging from seed germination, stem elongation, leaf expansion, and flowering to fruit development (Sun, 2010; Hu *et al.*, 2018). Genetic studies of GA-deficient and GA-response mutants have led to identification of key components in GA action and signaling. In rice, the GA receptor GIBBERELLIN-INSENSITIVE DWARF1 (GID1) interacts with the

aspartate–glutamate–leucine–leucine–alanine motif-containing DELLA protein SLENDER RICE1 (SLR1) to form a GA-GID1-DELLA complex in a GA-dependent manner. The GA-GID1 binding stimulates the interaction of DELLA with rice Skp1-Cullin1-F-box (SCF) SCF<sup>GID2</sup> protein, leading to the DELLA degradation via a ubiquitin-dependent pathway and the consequent activation of GA response (Ueguchi-Tanaka *et al.*, 2005, 2007; Hirano *et al.*, 2010). DELLAs are transcriptional factors in nuclei, whereas GID1 contains no apparent nuclear localization sequence, but how GID1 is localized to nuclei remains elusive.

Increasing results indicate that membrane lipids are rich sources for signaling messengers in plant response to hormones and stress conditions (Wang, 2004; Testerink & Munnik, 2005; Yao & Xue, 2018). Phospholipase D (PLD) hydrolyzes membrane lipids to generate phosphatidic acid (PA) that acts as lipid messengers (Mishra *et al.*, 2006; Zhang *et al.*, 2009; Yu *et al.*, 2010; Zhang *et al.*, 2012). PA can bind to target proteins to regulate biological processes (Min *et al.*, 2007; Guo *et al.*, 2012a; Yao *et al.*, 2013). The PA binding may enhance or inhibit the catalytic activity of target proteins (Zhang *et al.*, 2004; Guo *et al.*, 2012b; Anthony *et al.*, 2014), tether protein to subcellular membranes (Gao *et al.*, 2013; McLoughlin *et al.*, 2013), and/or promote the formation and/or stability of protein complex (Huang *et al.*, 2006; Li *et al.*, 2012, 2015). The rice genome contains 17 PLDs that can be subdivided into 3 groups, including the calcium-dependent phospholipid-binding C2-PLDs, the polyphosphoinositide-interacting PX/PH-PLDs, and a putative signal peptide-containing SP-PLD (Li *et al.*, 2007). PLDs play important and diverse roles in rice, such as responses to salt, cold, drought, and disease. OsPLD $\alpha$ 1 is involved in salt tolerance through mediating the H<sup>+</sup>-ATPase activity and transcription (Shen *et al.*, 2011). In addition, OsPLD $\alpha$ 1 affects cold stress response through its product PA regulating the expression of OsDREB1 (Huo *et al.*, 2016). Overexpression of PLD $\alpha$ 1 in upland rice improved drought tolerance by maintaining the photosynthetic apparatus integrity (Abreu *et al.*, 2018). Two chloroplast-localized PLDs, OsPLD $\alpha$ 4 and OsPLD $\alpha$ 5, regulate herbivore-induced direct and indirect defenses (Qi *et al.*, 2011). OsPLD $\beta$ 1 mediates disease response and stimulates abscisic

1 National Key Laboratory of Crop Genetic Improvement, Huazhong Agricultural University, Wuhan, China

2 The Rice Research Institute of Guangdong Academy of Agricultural Sciences, Guangzhou, China

3 Department of Biology, University of Missouri-St. Louis, St. Louis, MO, USA

4 Donald Danforth Plant Science Center, St. Louis, MO, USA

\*Corresponding author. Tel: +1 314 587 1419; E-mail: Liangshihu@sina.cn

\*\*Corresponding author. Tel: +1 314 516 6219; E-mail: swang@danforthcenter.org

\*\*\*Corresponding author. Tel: +86 027 87280545; E-mail: hongyy@mail.hzau.edu.cn

acid (ABA) signaling by activating the protein kinase SAPK to repress *GAMYB* expression and inhibit seed germination (Li *et al*, 2007b; Yamaguchi *et al*, 2009). Here, we report that PLD $\alpha$ 6 and PA mediate the subcellular localization of the GA receptor *GID1* and longitudinal cell growth in rice.

## Results

### Knockout of *PLD $\alpha$ 6* decreases GA sensitivity in rice

The rice genome has 17 putative PLDs that are designated as PLD $\alpha$  (8), PLD $\beta$ (2), PLD $\delta$ (3), PLD $\zeta$ (2), PLD $\kappa$ (1), and PLD $\phi$ (1). PLD $\alpha$ s, PLD $\beta$ s, PLD $\delta$ s, and PLD $\kappa$  contain the calcium/lipid-binding C2 domain and PLD $\zeta$ s have the PX and PH domains, whereas PLD $\phi$  has a signal peptide at the N-terminus. All C2-PLDs and PX/PH-PLDs contain two HKD (HxKxxxxD) catalytic motifs except that PLD $\alpha$ 7 has a mutation (RxKxxxxD) in the second HKD motif (Fig EV1A). PLD-C2 domain (calcium/lipid binding) that consists of eight strands was also found in PLD $\alpha$ s (Hong *et al*, 2016), and all the strands except the second share high homology between PLD $\alpha$ 6 and other PLD $\alpha$ s (Appendix Fig S1). PLD $\gamma$ s were identified in *Arabidopsis* but not in rice, whereas PLD $\kappa$  and PLD $\phi$  were in rice but not in *Arabidopsis*. Comparison of the amino acid sequences of OsPLDs with those of different plant species suggests that PLD $\gamma$ , PLD $\kappa$ , and PLD $\phi$  may be duplicated lately as they are not found in the moss *Physcomitrella patens* (es) or the lycophyte *Selaginella moellendorffii*, and they differ between the dicot *Arabidopsis thaliana* and monocot plants. By comparison, PLD $\alpha$ s and PLD $\delta$ s are found in lower and higher plant species, suggesting that they are original PLDs and conserved among plant species (Fig EV2).

Based on the rice CREP chip database (<http://crep.ncpgr.cn/crep-cgi/home.pl>), four *PLD $\alpha$ s* were highly differentially expressed in rice tissues (Fig EV1B). The transcript of *PLD $\alpha$ 6* and *PLD $\alpha$ 5* was detected primarily in stems and roots, respectively, whereas that of *PLD $\alpha$ 2* and *PLD $\alpha$ 8* was detected mainly in inflorescence. In comparison, the transcript of *PLD $\alpha$ 1* and *PLD $\alpha$ 3* was high at almost all tissues (Fig EV1B). To verify the results, we performed real-time PCR (qRT-PCR) and found that *PLD $\alpha$ 6* transcript was highest in stems, while it was detectable in other seedling tissues, including leaves, leaf sheath, roots, and inflorescence. In addition, the transcript level of *PLD $\alpha$ 6* in leaves was increased in response to GA $_3$  and naphthylacetic acid (NAA), but not to kinetin (KT), whereas that of *PLD $\alpha$ 3* was increased in response to all the hormones tested (Fig EV1C).

To investigate the function of rice PLDs, T-DNA-insertional mutants for various PLDs, including *pld $\alpha$ 1*, *pld $\alpha$ 3*, *pld $\alpha$ 6*, and *pld $\delta$ 2*,

were isolated and tested for sensitivity to ABA, indole-3-acetic acid (IAA), and GA $_3$ . The *pld $\alpha$ 6* mutant was less sensitive to GA $_3$  than wild type (WT) (Fig EV3). To confirm the function of PLD $\alpha$ 6, we genetically complemented the *pld $\alpha$ 6* mutant with the native *PLD $\alpha$ 6* (*PLD $\alpha$ 6-COM*) (Fig 1A). The expression level of *PLD $\alpha$ 6* in *pld $\alpha$ 6* and *PLD $\alpha$ 6-COM* was verified by quantitative real-time PCR. The lack of *PLD $\alpha$ 6* transcript in the mutant indicates that *pld $\alpha$ 6* is a knockout (KO) mutant, whereas *PLD $\alpha$ 6-COM* restored *PLD $\alpha$ 6* expression in the mutant to that of WT plants (Fig 1B).

WT, *pld $\alpha$ 6*, and COM plants displayed no overt morphological alterations under normal growth conditions at the early stage (4-leaf-old) of rice. However, at the mature stage, the longitudinal growth including plant height, panicle length, and flag leaf length in the *pld $\alpha$ 6* mutant was significantly reduced as compared to WT and COM when plants were grown in the field (Appendix Fig S2). In addition, *pld $\alpha$ 6* was delayed in flowering time reduced in spikelet numbers compared to WT and COM plants, whereas tiller number and leaf width were similar among WT, *pld $\alpha$ 6*, and COM plants (Appendix Fig S2).

To further characterize the GA response, five-day-old seedlings germinated under normal conditions were transferred to liquid media containing 0, 0.1, 1, and 10  $\mu$ M GA $_3$ . After one week, WT and *pld $\alpha$ 6* plants displayed significant differences in seedling length and fresh weight in GA $_3$ -containing media (Fig 1C). The seedlings of *pld $\alpha$ 6* were shorter and lighter than those of WT (Fig 1D and E). In the presence of 0.1  $\mu$ M GA $_3$ , the plant height of *pld $\alpha$ 6* seedlings was increased by 12%, whereas that was increased by 30% in WT and COM, compared to corresponding plants without GA treatments. With increasing GA concentrations, the differences between *pld $\alpha$ 6* and WT became greater in the GA's growth-promoting effect. These results indicate that the loss of PLD $\alpha$ 6 decreases GA $_3$  sensitivity in rice.

### OsPLD $\alpha$ 6 hydrolyzes phospholipids and affects PA content and lipid composition

To test whether *PLD $\alpha$ 6* encodes a functional PLD, the *PLD $\alpha$ 6* cDNA was tagged at the C-terminus with polyhistidine (6xHis) and expressed in *E. coli* (Fig 2A). Purified PLD $\alpha$ 6 displayed Ca $^{2+}$ -dependent hydrolysis of phospholipids with the highest activity at the mM levels of Ca $^{2+}$  toward phosphatidylcholine (PC). PLD $\alpha$ 6 also hydrolyzed phosphatidylethanolamine (PE), phosphatidylglycerol (PG), and phosphatidylserine (PS), and the highest activity was detected with PE (Fig 2B, Appendix Fig S3). The apparent production of PA associated with the empty vector pET28-His control could be due to background contaminants in the sample purified from the *E. coli* harboring the empty vector. To correct the background PA,

**Figure 1. Decreased GA response in *PLD $\alpha$ 6*-KO plants.**

- T-DNA insertion site in the *PLD $\alpha$ 6* gene and the complementation construct introduced into the T-DNA insertion mutant. Boxes denote exons and lines introns.
- PLD $\alpha$ 6* transcript in WT, *pld $\alpha$ 6*, and complementation line (*PLD $\alpha$ 6-COM*). Leaf samples from 4-leaf stage rice (Dongjin background) were collected, and the expression levels of *PLD $\alpha$ 6* were analyzed by normalizing to that of *GAPDH*. Values are means  $\pm$  SD ( $n = 3$  biological repeats).
- Seedling phenotype under GA treatment. After germination, five-day-old seedlings with the same growth stage were transferred to 0.5 MS liquid media without or with different concentrations of GA $_3$ . PA from soybean was added to the media at a final concentration of 20  $\mu$ M. Pictures were taken 7 days after transfer. The horizontal red line separates different plants, and the vertical red scale bar represents 2 cm.
- Seedling length of WT, *pld $\alpha$ 6*, COM, and PA-treated plants grown on 0, 0.1, 1, and 10  $\mu$ M GA $_3$  for 7 days. Values are means  $\pm$  SD ( $n = 15$  plants) from one representative of three independent experiments.
- Fresh weight of 10 seedlings of WT, *pld $\alpha$ 6*, COM, and PA-treated plants grown on 0, 0.1, 1, and 10  $\mu$ M GA $_3$  for 7 days. Values are means  $\pm$  SD ( $n = 15$  plants) from one representative of three independent experiments.

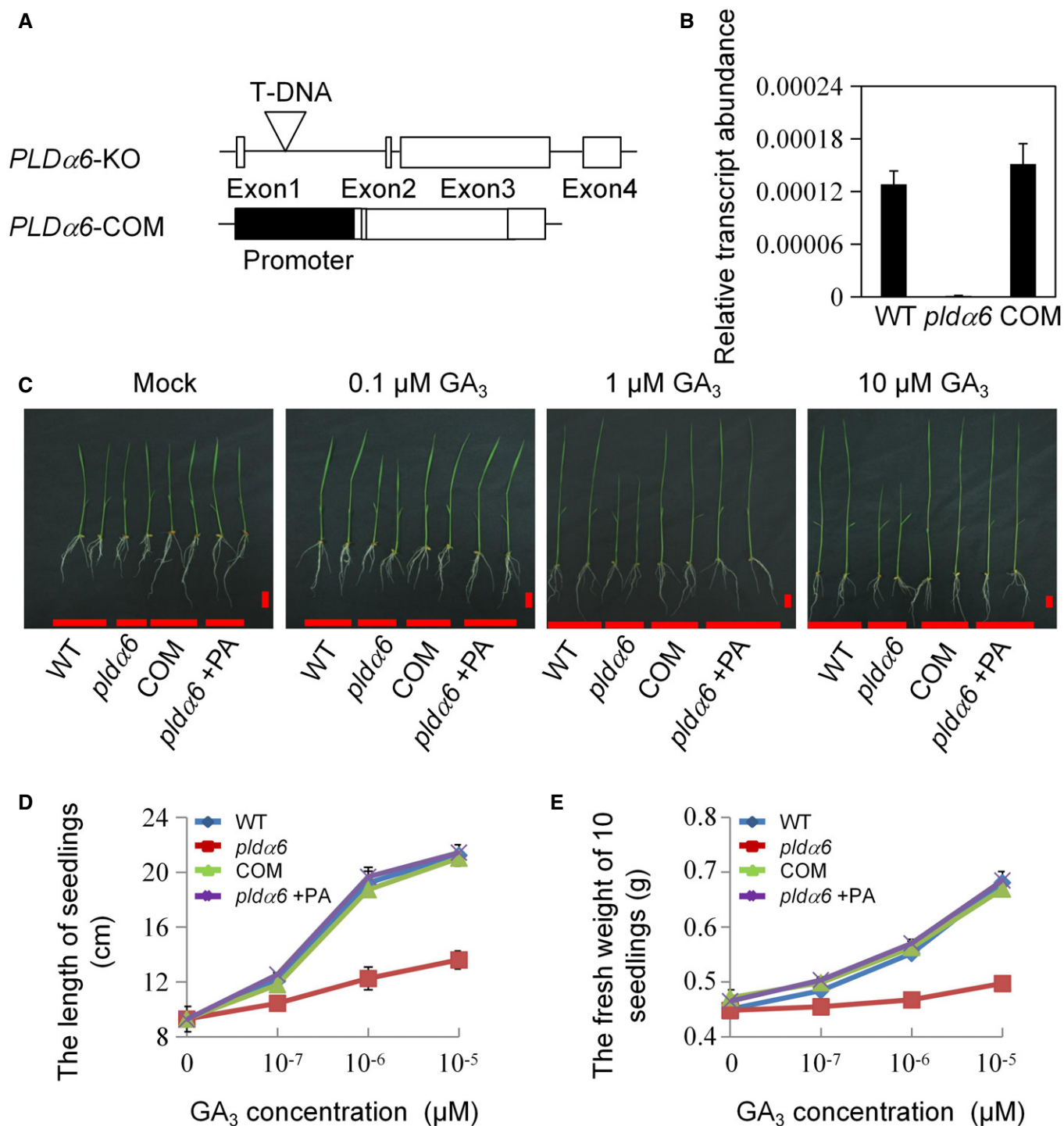
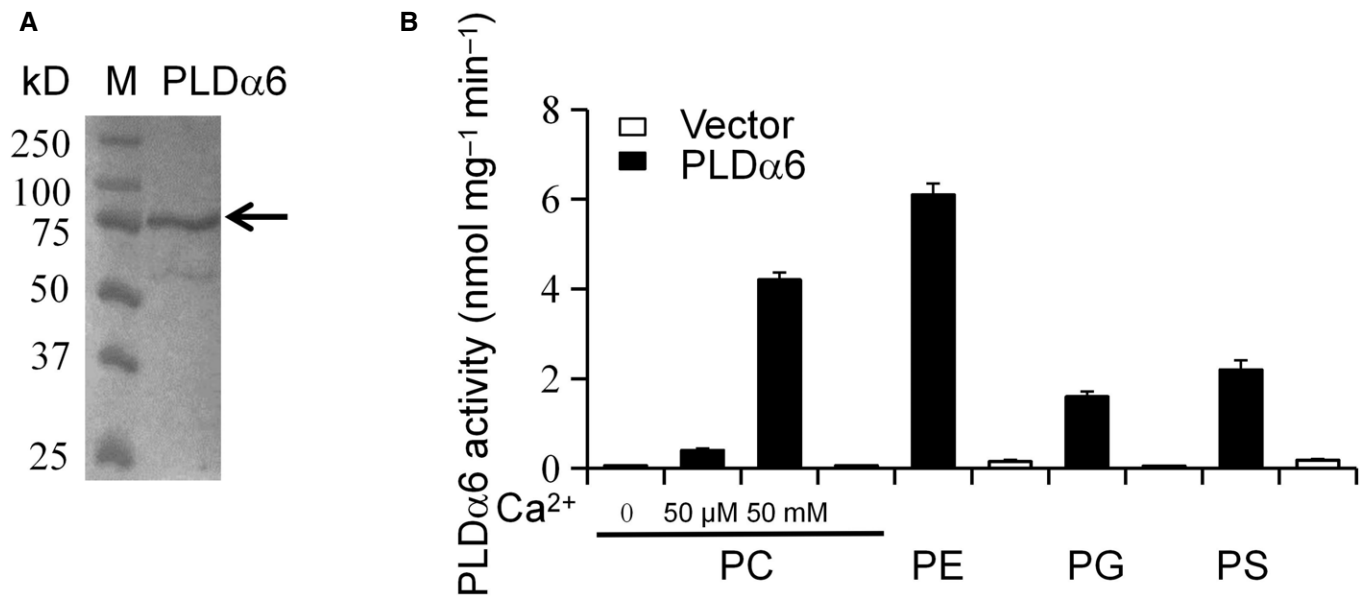


Figure 1.

we determined PA produced by subtracting PA presented with empty vector from PA produced in the presence of PLD $\alpha$ 6.

To examine the effect of PLD $\alpha$ 6 on lipid metabolism in rice plants, we analyzed lipids from 2-week-old leaves of WT, *pldα6* and COM, using mass spectrometry. The level of monogalactosyldiacylglycerol (MGDG) and digalactosyldiacylglycerol (DGDG) was similar among *pldα6*, WT, and COM plants with and without the GA<sub>3</sub> treatment. Without GA, PA content in *pldα6* plants was ~70% of that in

WT plants, whereas the level of PC (130% of WT) and PE (115% of WT) was significantly higher in *pldα6* than that in WT and COM plants (Fig 3A). The decreased PA level in *pldα6* was due to primarily the decrease in 34-carbon and 36-carbon PA species, whereas the increased PC and PE resulted from elevated 34- and 36-carbon species (Fig 3B). The results indicate that PLD $\alpha$ 6 contributes to the production of basal PA and that PLD $\alpha$ 6 prefers PC and PE as the main substrates *in vivo* under normal condition. In the presence of



**Figure 2. PLD $\alpha$ 6 production and hydrolysis of phospholipids.**

A Immunoblotting of His-tagged PLD $\alpha$ 6 (arrow) expressed in *E. coli* as separated on a 10% SDS-PAGE and blotted to a membrane.

B Lipid hydrolyzing activity assayed in the presence of different phospholipids using purified PLD $\alpha$ 6 from *E. coli*. Solid bars are activities assayed using purified PLD $\alpha$ 6, whereas open bars were empty vector control that used an equal volume of eluents from bacteria containing the empty vector that was identically processed as those expressing PLD $\alpha$ 6. Values are means  $\pm$  SD ( $n = 3$  biological replicates).

GA, the content of PE (118% of WT) and PS (194% of WT) in *pldx6* was significantly higher, whereas that of PA in the mutant was lower than that of WT (Fig 3A). The decreased PA in *pldx6* was due primarily to reduced 34:2-, 34:3-, 36:4-, and 36:5-PA species, whereas increased PE in *pldx6* resulted from elevating 34:2-, 34:3-, 36:4-, and 36:5-PE species (Fig 3B). These data indicate that PE and PS may be the main source of PA in response to the GA<sub>3</sub> treatment.

#### PA promotes GA response and interacts with GA receptor GID1

To probe how PLD $\alpha$ 6 affects GA response, we tested whether the PLD lipid product PA could restore *pldx6*'s GA<sub>3</sub> response to that of WT. In the presence of GA<sub>3</sub> and PA, the length and fresh weight of *pldx6* seedlings were comparable to those of WT and COM (Fig 1C–E). The cell length in the second leaf sheath of *pldx6* was 60% of that WT and COM in the presence of 10  $\mu$ M GA<sub>3</sub> and was recovered to that of WT when PA was supplied to the growth media (Appendix Fig S4A and B). The PA restoration of *pldx6* seedling growth to that of WT suggests that PLD $\alpha$ 6-produced PA is likely responsible for the effect of PLD $\alpha$ 6 on GA-promoted growth.

To explore how PA mediates rice response to GA, we examined potential interactions between PA and GID1 and SLR1, two major components of GA perception and signal transduction in rice. Using the same amount of OsGID1 and OsSLR1 proteins produced and purified from *E. coli* (Fig 4A), GID1 displayed a strong binding signal to PA, whereas SLR1 and control pET28 protein gave no signal on a lipid-protein blotting assay. No signal was detected for binding between GID1/SLR1 and other phospholipids, such as PC, PE, PG, and PS (Fig 4B). In addition, liposome binding was performed to verify the interaction between PA and OsGID1. GID1

was co-precipitated with liposomes consisting of PA: PC (1:3 molar ratio), and the amount of GID1 associated with liposomes increased with increasing amounts of PA in the liposomes. In contrast, liposomes with PC alone failed to bind to GID1. Similar to the lipid blotting, no PA binding with SLR1 was detected in the liposomal assay (Fig 4C).

Furthermore, the PA-GID1 binding was verified by surface plasmon resonance (SPR). In the representative sensorgram, a strong increase in response units (RUs) occurred when PA-containing liposomes were infused to a GID1-containing chip PA, whereas only a slight increase was detected when liposomes containing PC, PS, or PG-only were injected (Appendix Fig S5). Association ( $k_a$ ) and dissociation ( $k_d$ ) constants for PA were 117 M<sup>-1</sup> s<sup>-1</sup> and 1.37  $\times$  10<sup>-5</sup> s<sup>-1</sup>, respectively, with a binding affinity ( $K_D = k_d/k_a$ ) at 1.2  $\times$  10<sup>-7</sup> M. By contrast,  $k_a$  and  $k_d$  for PC were 60.9 M<sup>-1</sup> s<sup>-1</sup> and 7.17  $\times$  10<sup>-4</sup> s<sup>-1</sup>, respectively, resulting in a  $K_D$  of 1.2  $\times$  10<sup>-5</sup> M. Thus, the binding affinity of GID1 to PA was  $\sim$ 100-fold greater than that of PC. The results suggest that GID1 binds to PA *in vitro* with a high affinity.

#### Arg79 and Arg82 of GID1 are required for PA binding

To identify the protein region involved in PA binding, several deletion mutants of GID1 were constructed and expressed in *E. coli*. Rice GID1 shares a high homology with hormone-sensitive lipase (HSL) which contains three conserved domains, HGG motif, GX SXG motif, and a catalytic triad (Ueguchi-Tanaka et al, 2005). The N-terminal truncated mutants covering residues 1–119 (F1) and 1–138 (F2) displayed the strongest binding signal to PA. The C-terminal truncated mutant containing 51 to 354

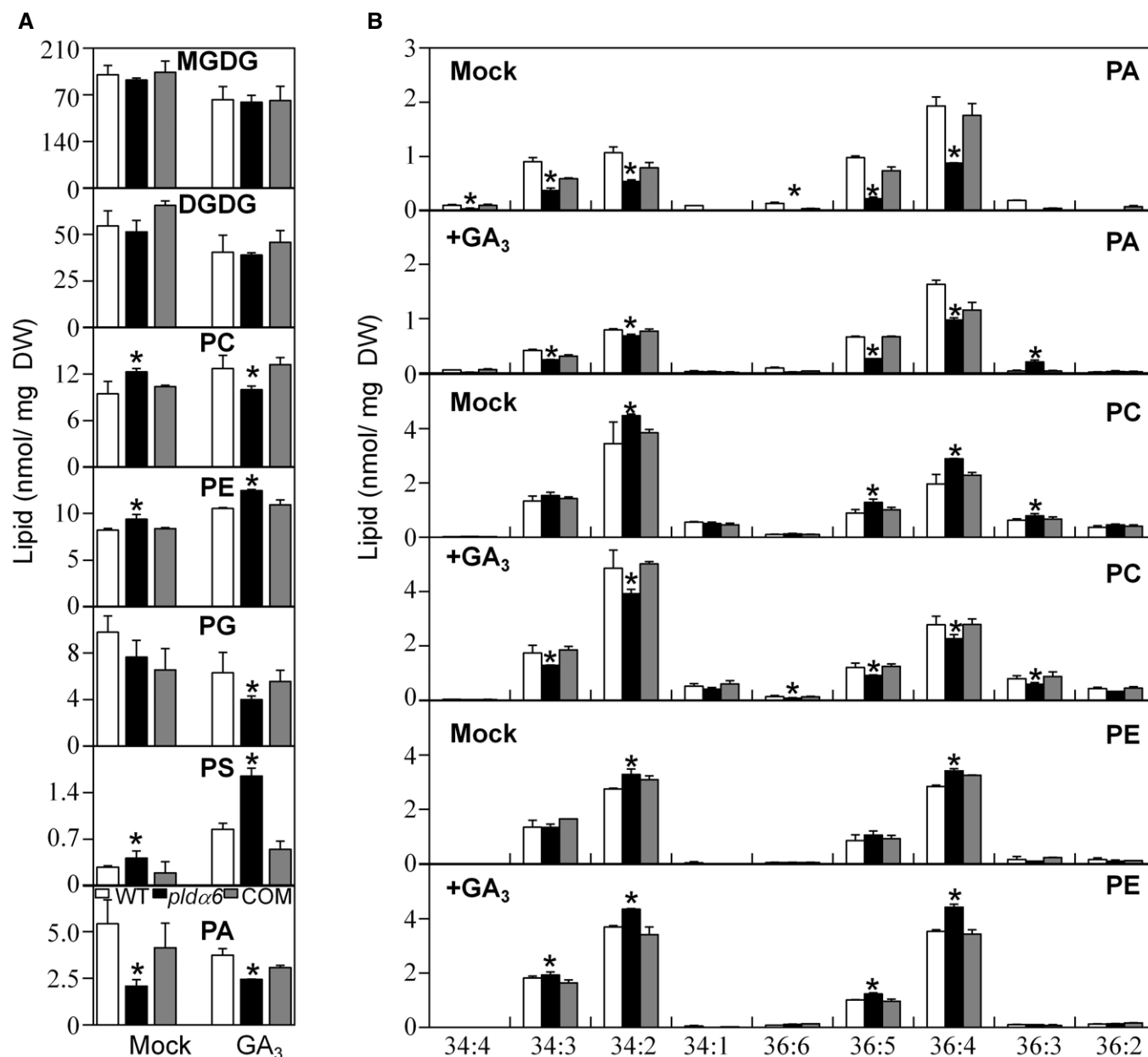


**Figure 3. Effect of *PLDα6*-KO on lipid changes in response to GA.**

**A** Total lipid levels in WT, *pldα6*, and COM without and with 10  $\mu$ M GA<sub>3</sub>. Leaf samples (15 seedling each) from 4-leaf stage rice (Dongjin background) were collected, and lipids were extracted and profiled using ESI-tandem mass spectrometry. Values are means  $\pm$  SD ( $n = 3$  biological replicates). MGDG, monogalactosyldiacylglycerol; DGDG, digalactosyldiacylglycerol; PC, phosphatidylcholine; PE, phosphatidylethanolamine; PG, phosphatidylglycerol; PS, phosphatidylserine; and PA, phosphatidic acid.

**B** Phospholipid species in WT, *pldα6*, and COM. Leaf samples (15 seedling each) from 4-leaf stage rice (Dongjin background) were collected and, the different phospholipid species including carbon number and double bond number were determined. Values are means  $\pm$  SD ( $n = 3$  biological replicates). GA<sub>3</sub> was dissolved in ethanol, and seedlings treated with the same ethanol concentration were used as control.

Data information: In panels A and B, \* denotes significant at  $P < 0.05$  compared with WT under the same treatment based on Student's *t*-test.

amino acid (aa) (F5) showed PA binding, whereas no binding was found between PA and the shorter C-terminal fragments covering 139–354 aa (F4) and 120–354 aa (F3) (Fig 4D and E). These results suggest that the PA-binding site is located in the N-terminal 51–119 residues of GID1.

Basic amino acid residues involved in binding to PA have been documented (Zhang *et al*, 2004; Testerink & Munnik, 2005; Awai

*et al*, 2006; Wang *et al*, 2006). There are six Arg residues in the putative PA-binding region covering from 51 to 119 aa (Fig 4F). Therefore, we generated eight mutants with the basic Arg residues substituted with Ala, including six single mutants GID1<sub>R51A</sub>, GID1<sub>R52A</sub>, GID1<sub>R58A</sub>, GID1<sub>R79A</sub>, GID1<sub>R82A</sub>, and GID1<sub>R98A</sub> and two double mutants GID1<sub>R51AR52A</sub> and GID1<sub>R79AR82A</sub>. All GID proteins with a single-site mutation still exhibited binding to PA as did GID

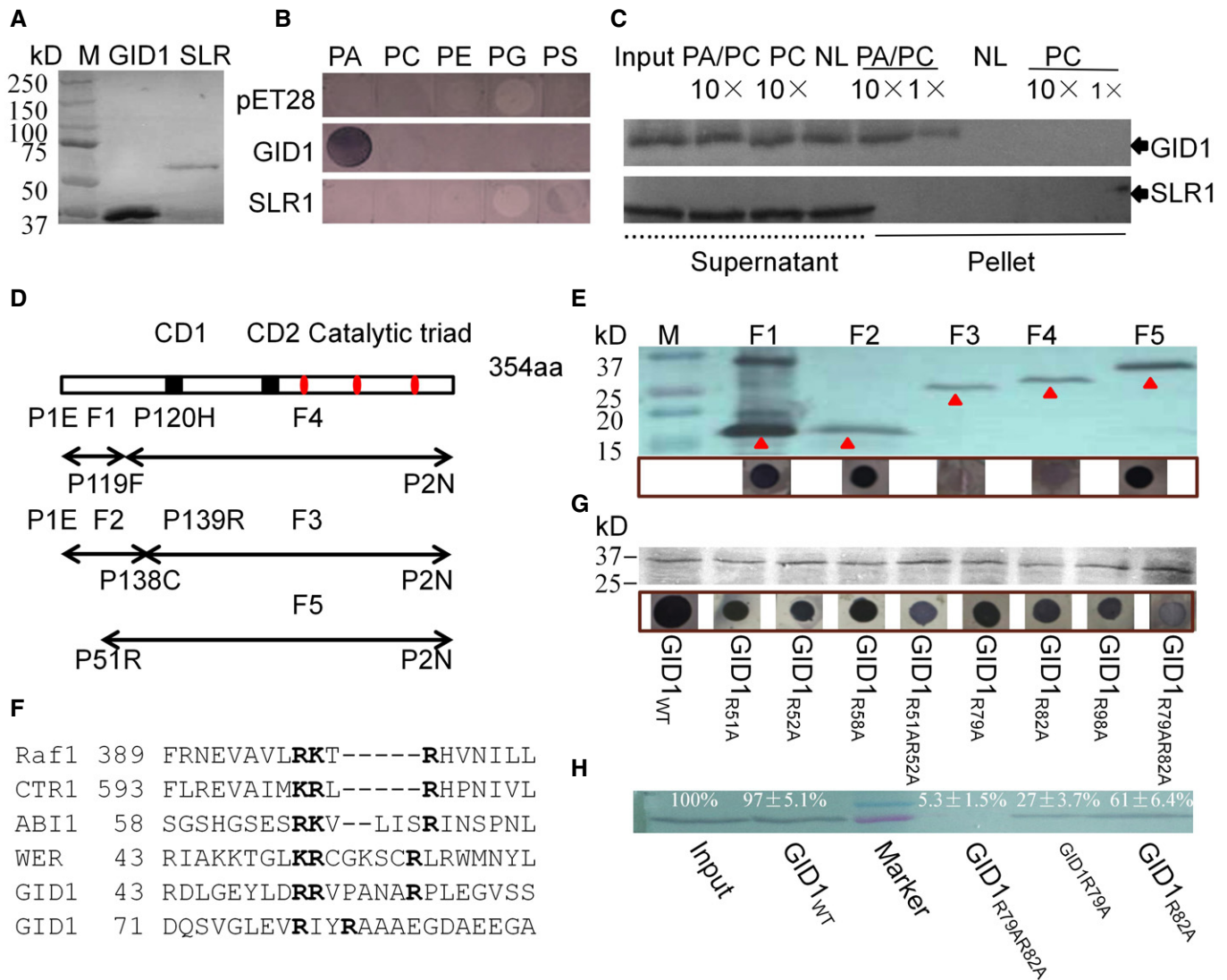


**Figure 4. PA-GID1 interaction and amino acid residues involved in the binding.**

**A** Immunoblotting of His-GID1 and His-SLR1 expressed in *E. coli*.

**B** Lipid-protein blotting assay of PA, PC, PE, PG, and PS with GID1 and SLR1. Lipids (0.5  $\mu$ g) were spotted on nitrocellulose strips. PA, PC, PE, and PG were from egg yolk, and PS was from porcine brain. Purified proteins (GID1 and SLR1, 0.5 mg/ml) were used, followed by immunoblotting with anti-His-tag antibodies and color development.

**C** Liposomes were made from di18:1-PC only or di18:1-PA/PC (PA:PC = 1:3 mole ratio). 1 $\times$  and 10 $\times$  refer to the concentration of PC or PA/PC liposomes used. NL, no liposome was added to the binding mixture.

**D** Schematic diagram showing serial deletions of GID1. GID1 fragments were expressed in *E. coli* and used for defining the PA-binding region. CD1/2 denote conserved domain HGG and GXSGC. Catalytic triad including three conserved amino acids of GID1, S, D, and H (vertical red bars).

**E** Immunoblotting of His-GID1 proteins using constructs shown in (D). Proteins were separated by SDS-PAGE, followed by immunoblotting with anti-His-tag antibodies. The PA-binding activity of different truncation mutations was analyzed by fat immunoblotting. The red arrowheads indicate truncated proteins with different molecular weights.

**F** Sequence alignment of the PA-binding fragment of GID1 with that of the PA-binding motifs in chicken Raf1, abscisic acid-insensitive 1 (ABI1), constitutive triple response1 (CTR1), and werewolf (WER) from *Arabidopsis*. Residues in bold are basic, potentially involved in PA binding and were mutated to Ala in GID1.

**G** Immunoblotting of His-GID1 mutants and lipid immunoblotting of PA binding by GID1 mutant proteins on a filter.

**H** Liposomal binding of GID1 proteins to PA. Liposomes were made from di18:1-PA/PC (PA:PC = 1:3 mole ratio). Liposomal associated proteins were subjected to SDS-PAGE and immunoblotting using anti-His antibodies. The band intensity was analyzed by ImageJ, and the intensity of input was set as 100%.

without mutation. However, the mutant GID1<sup>R79AR82A</sup>, but not GID1<sup>R51AR52A</sup>, lost PA binding (Fig 4G and H). The results suggest that Arg79 and Arg82 of GID1 are two key amino acid residues for PA binding.

#### PLD $\alpha$ 6 and PA promote OsGID1's nuclear localization

To determine how PLD $\alpha$ 6 and PA modulate GID1 functions, we examined the effect of PLD $\alpha$ 6 and PA on the nuclear localization of

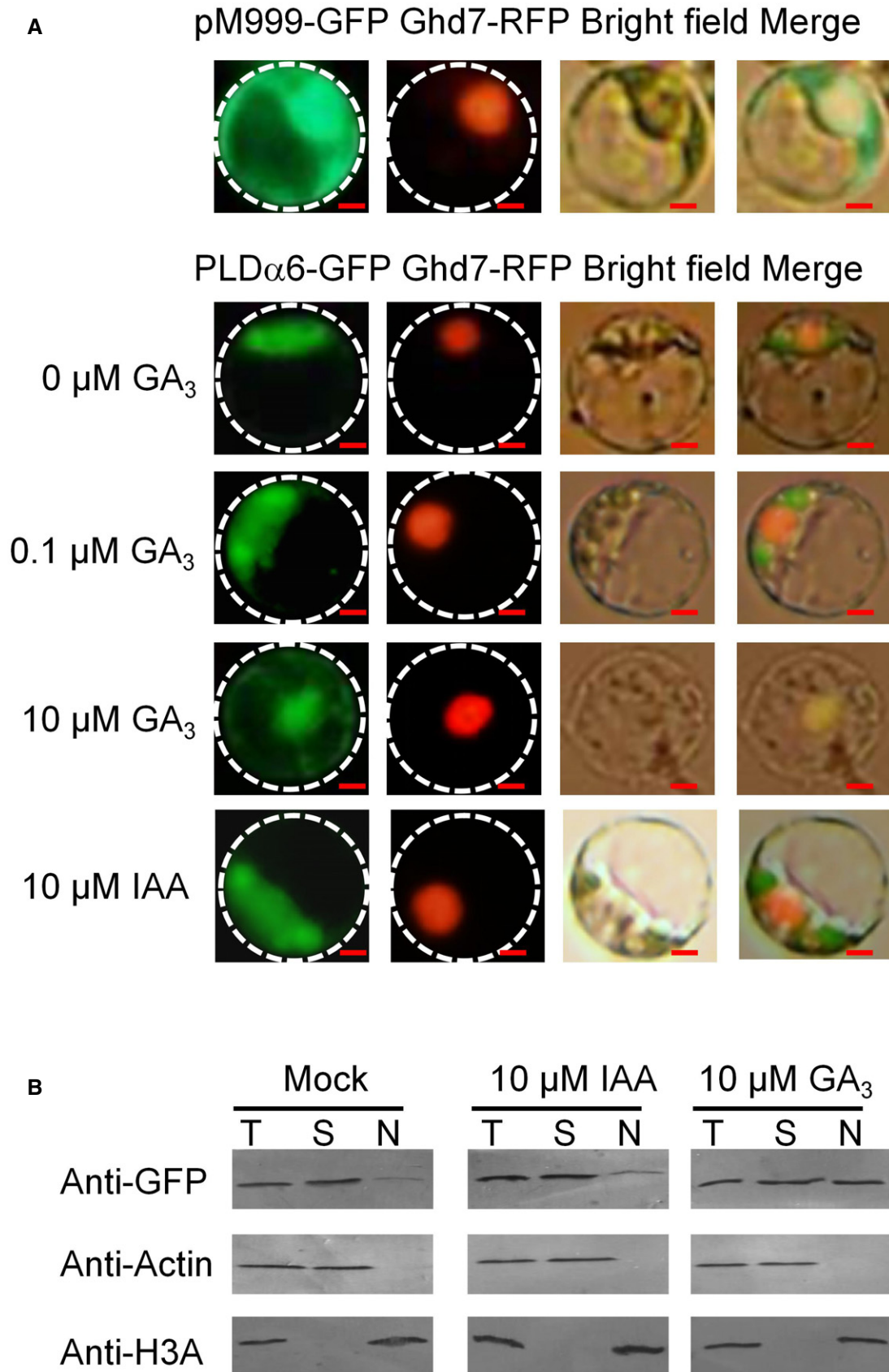
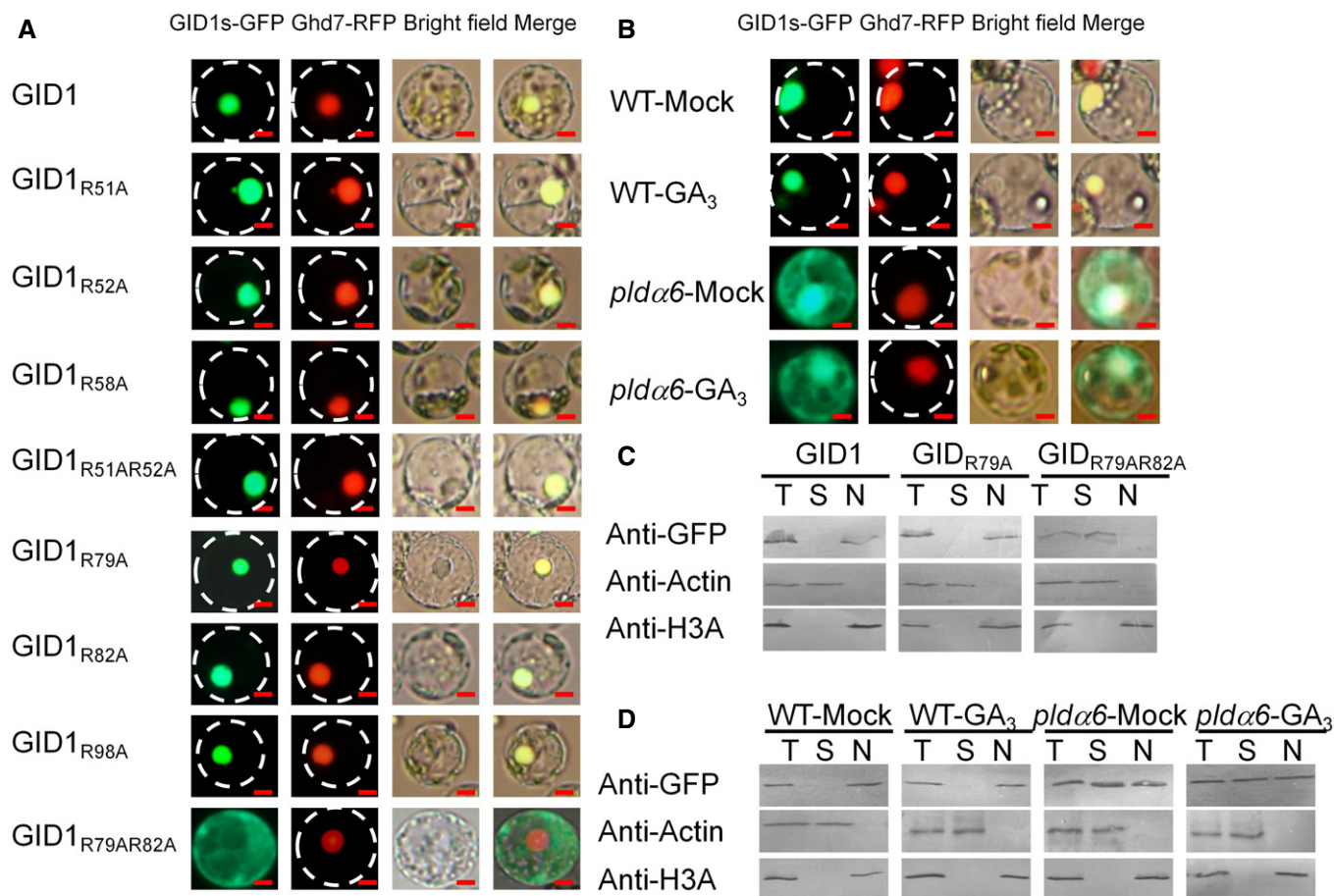


Figure 5.

**Figure 5. Subcellular localization of PLD $\alpha$ 6.**

A PLD $\alpha$ 6-GFP distribution in rice protoplasts with different concentrations of GA<sub>3</sub> or IAA. Protoplasts from 12-day-old rice (ZH11 background) leaf sheath tissue were collected. Rice protoplasts were transfected with pM999-PLD $\alpha$ 6 for 12 h. After that, GA<sub>3</sub> or IAA was added to protoplasts, and 2 h later, confocal images of protoplasts are shown. pM999-GFP refers to the empty vector with GFP only that was transformed as control and Ghd7-RFP was a nucleus marker. Scale bar = 10  $\mu$ m.

B Immunoblotting of PLD $\alpha$ 6 in subcellular fractions. Total (T), soluble (S), and nuclear (N) proteins were isolated from PLD $\alpha$ 6:GFP expressed in rice protoplasts treated with 10  $\mu$ M GA<sub>3</sub> or IAA. Equal amount of each sample was loaded for SDS-PAGE and blotting.

**Figure 6. Effect of PLD $\alpha$ 6-KO on subcellular localization of GID1.**

A Protoplasts from 12-day-old rice (ZH11 background) leaf sheath tissue were collected, and protoplasts were transfected with pM999-GID1 and mutation constructs and imaged 12 h after transfection. All confocal images were scanned using similar laser gain and offset settings. Bars = 10  $\mu$ m.

B Subcellular location of GID1 in WT and *pld $\alpha$ 6* protoplasts with or without GA<sub>3</sub> treatments. Cells for 12 h after transformation were treated with or without 10  $\mu$ M GA<sub>3</sub> for 2 h. Bars = 10  $\mu$ m.

C Immunoblotting of subcellular fractions of GID1 and mutations expressed in rice protoplasts. Total (T), soluble (S), and nuclear (N) protein fractions were isolated from protoplasts for 12 h after transformation. Equal amounts of proteins from each sample were loaded.

D Immunoblotting of subcellular fractions of GID1 expressed in WT and *pld $\alpha$ 6* protoplasts. After 2-h treatment with 10  $\mu$ M GA<sub>3</sub>, total (T), soluble (S), and nuclear (N) protein fractions were isolated from 10 samples of protoplasts. Equal amount of each sample was loaded for SDS-PAGE and immunoblotting.

GID1. We first assessed the subcellular localization of PLD $\alpha$ 6, using a PLD $\alpha$ 6 fused with the green fluorescent protein (GFP) at the C-terminus transiently expressed in rice protoplasts. PLD $\alpha$ 6-GFP was detected in both nucleus and cytosol, and its nuclear localization was enhanced by GA supplementation. In contrast, the IAA treatment did not change the intracellular distribution of PLD $\alpha$ 6-GFP (Fig 5A). Subcellular fractionation also showed that more PLD $\alpha$ 6

was detected in the nuclear fraction when cells were treated with GA<sub>3</sub> (Figs 5B and EV4A and B).

To test whether PLD $\alpha$ 6 and PA affect GID1's subcellular localization, GID1 fused with GFP was expressed in the protoplasts isolated from seedlings of WT and *pld $\alpha$ 6*. Rice Ghd7 (a PSEUDO-RESPONSE REGULATOR 7-like protein) was used as a nuclear localization marker (Xue et al, 2009). GID1 in WT protoplasts was localized in the



nucleus, whereas it was localized in both nucleus and cytosol of *pldα6* protoplasts. The presence of added GA<sub>3</sub> did not affect the GID1's subcellular distribution in either WT or *pldα6* cells (Fig 6B and D).

To further determine whether the PA-GID1 interaction is required for GID1's nuclear localization, we expressed the non-PA-binding GID1<sub>R79AR82A</sub> mutant fused with GFP and GID1-GFP, as well as six single GID mutants and GID1<sub>R51AR52A</sub> fused with GFP in rice protoplasts. The GFP signal in the mutant GID1<sub>R79AR82A</sub>-GFP was detected in the cytosol but not in the nucleus (Fig 6A). In contrast, the GFP signal in cells expressing GID1-GFP, six single mutant- and GID1<sub>R51AR52A</sub>-GFP fusions was co-localized with the nuclear marker Ghd7. To verify the subcellular distribution, we performed subcellular fractionation of rice protoplasts, followed by immunoblotting, and verified the loss of nuclear localization of the GID1<sub>R79AR82A</sub> mutant (Fig 6C). In addition, we transiently expressed GID1<sub>R79AR82A</sub>-GFP and GID1-GFP in tobacco leaves and verified the loss of GID1<sub>R79AR82A</sub>'s nuclear localization (Fig EV5A and B). These data suggest that PLDα6 and PA are important for the subcellular distribution of GID1 and that the PA-GID1 binding is required for its nuclear localization.

#### PLDα6 promotes SLR1 degradation in response to GA

In the GA signal transducing process, the GA receptor GID1 interacts with DELLA proteins, such as SLR1, and GA promotes the degradation of SLR1, activating GA response (Ueguchi-Tanaka et al, 2005, 2007; Hirano et al, 2010). To test the effect of PA-GID1 interaction on the degradation of downstream target SLR1, we constructed the SLR1-GFP in the plant transient expression vector pM999-GFP and transformed the construct into rice protoplasts. SLR1-GFP was localized to nuclei in WT and *pldα6* cells with or without GA treatments. However, the addition of GA promoted SLR1 degradation, but GA-promoted SLR1 degradation in *pldα6* was less than that in WT (Fig 7A). The SLR1-GFP signal in WT cells was decreased for 3 h after a GA<sub>3</sub> treatment, and no GFP signal was detected after 9 h of a GA treatment. In comparison, the GFP signal in *pldα6* cells still remained high 9 h after the GA<sub>3</sub> treatment, being one-third of non-GA<sub>3</sub> treatment control (Fig 7A). In addition, we verified the effect of PLDα6 on decreased SLR1 degradation by immunoblotting because more SLR1 protein was detected in *pldα6* cells than WT cells after the GA treatment (Fig 7B). Those results from microscopic and immunoblotting observations both suggest that PLDα6 promotes SLR1 degradation in response to GA.

In addition, we tested whether the knockout of *PLDα6* affected the expression of genes involved in GA signaling and metabolism. Without added GA, the transcript level of *GID1* and *SLR1* was higher in WT than *pldα6* (Appendix Fig S6). In response to a GA treatment, the transcript level of *GID1* decreased, whereas that of *SLR1* increased in WT and *pldα6*. Gibberellin 3β-hydroxylase 1 (*GA3OX1*) and gibberellin 20-oxidase 1 (*GA20OX1*) are involved in the production of bioactive Gas, whereas gibberellin 2-oxidase 1 (*GA2OX1*) catalyzes the inactivation of GAs. There was no difference between WT and *pldα6* in the transcript level of *GA3OX1* or *GA20OX1* with or without GA treatments. Without GA treatment, the transcript level of *GA2OX1* was slightly lower in *pldα6* than WT but with added GA, the level of *GA2OX1* was similar in *pldα6* and WT (Appendix Fig S6). With the limited number of genes tested, the results could mean that the knockout of *PLDα6* did not alter significantly the expression of genes involved in GA metabolism.

## Discussion

The PLD family has multiple members, and several PLDs are involved in plant response to hormones in *Arabidopsis*, such as PLDα1 and PLDδ in response to ABA (Sang et al, 2001; Zhang et al, 2004) and PLDζ2 in auxin (Li & Xue, 2007). The PLDs are more diverse in rice than *Arabidopsis* (Li et al, 2007), but their roles and molecular mechanisms of action remain largely unknown. Results of this study indicate that rice PLDα6 plays a positive role in longitudinal growth through its PA-mediated GA response. PA binds to the GA receptor GID1 that is found in the nucleus (Ueguchi-Tanaka et al, 2005). GID1 contains no apparent nuclear localization sequence (NLS), but how GID1 is localized to nuclei remained unknown. Our study showed that the loss of PLDα6 compromised the nuclear localization of GID1 and that the PA-GID1 interaction is required for GID1's nuclear localization in rice protoplasts. Previously, PA was found to facilitate the nuclear localization of a R2R3 MYB transcription factor involved in root hair formation in *Arabidopsis*, but enzymes responsible for that PA production remained unknown (Yao et al, 2013).

In this study, we found that PLDα6 was translocated from cytosol to nuclei in response to GA treatment. Nuclear membranes contain various phospholipids, such as PC, PE, and PS that are substrates for PLDα6 to produce PA. Thus, the activity of PLDα6 could potentially increase PA in the nuclear envelope in response to GA. However, direct measurement of GA-induced PA increase in the nuclear envelope is technically challenging because fractionation would activate lipolytic enzymes, such as PLDs, thus altering lipid composition. The functional significance of PA in GA response is supported by the supplementation of PA that restored the normal GA response in of the *PLDα6*-KO mutant. In addition, the requirement of PA-GID1 binding in GID1 localization further supports the PA function. Those results indicate PLDα6 positively mediates GA via the lipid mediator PA. PA may tether GID1 to the nuclear membrane to facilitate GID1's translocation from cytosol to the nucleus.

Comparative lipid analysis between WT and *pldα6* indicates that PLDα6 is involved in the basal and GA-induced PA production. However, it is possible that other enzymes are involved in PA production in response to GA. Specifically, the transcript level of *PLDα3* is induced several-fold by GA in leaves and the highest in stem relative to other tissues. In addition, WT and *pldα6* plants displayed no overt growth difference at early seedling stages, suggesting also potential functional redundancy between PLDα6 and other PLDs. However, mature *pldα6* plants are shorter than WT plants, which could mean that PLDα6 is a major mediator of the GA response and that the functional redundancy could occur more at early than mature growth stages. The transcript levels of genes involved in GA metabolism displayed a similar change in WT and *pldα6* in response to GA<sub>3</sub>. The result implicates that the decreased GA response in the *pldα6* mutant did not directly result from altered GA metabolism in plants. On the other hand, with or without GA treatments, the transcript level of *GID1* and *SLR1* in *pldα6* was both lower than that in WT. This decrease could mean that due to subdued GA signaling in the *pldα6* mutant, less GID1 and SLR1 proteins are needed.

Based on the results, we propose a model of interaction between PLDα6/PA and GID1 in GA signaling (Fig 8). PLDα6 is translocated

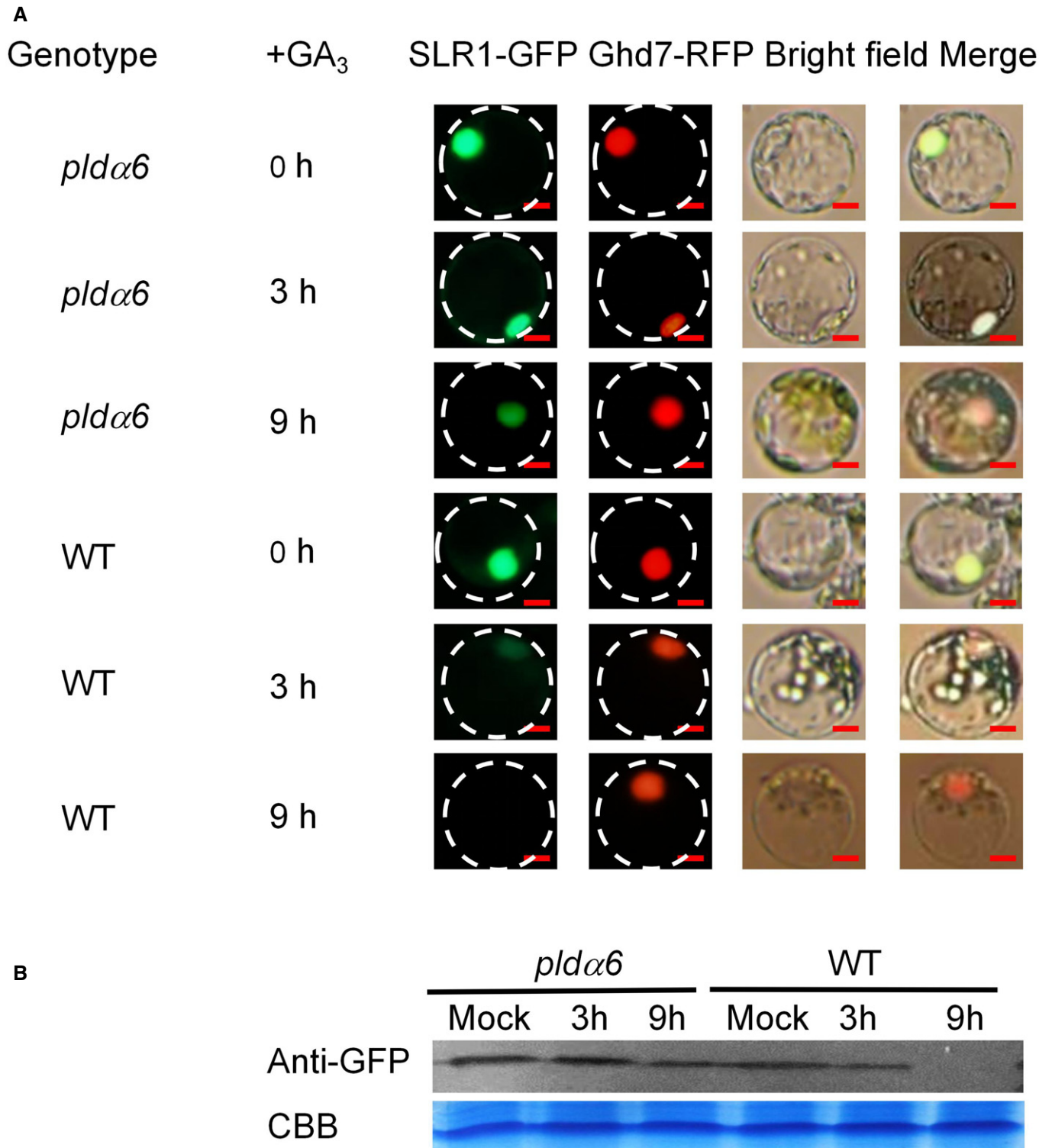


**Figure 7. SLR protein stability in WT and *pldα6* protoplasts.**

A Protoplasts of WT and *pldα6* from 12-day-old stage leaf sheath were collected and transfected with a pM999-SLR1 construct, incubated for 12 h, and then treated with 10 μM GA<sub>3</sub> for 0, 3, and 9 h. The first column, fluorescence from GFP; the second, red fluorescence from the nucleus marker Ghd7; the third, bright field; and the fourth, overlay of the three channels. All confocal images were scanned using similar laser gain and offset settings. Bars = 10 μm.

B Immunoblotting of SLR1-GFP proteins from protoplast cells. Equal amounts of proteins from each sample were used for SDS-PAGE, followed by immunoblotting with anti-GFP antibodies.

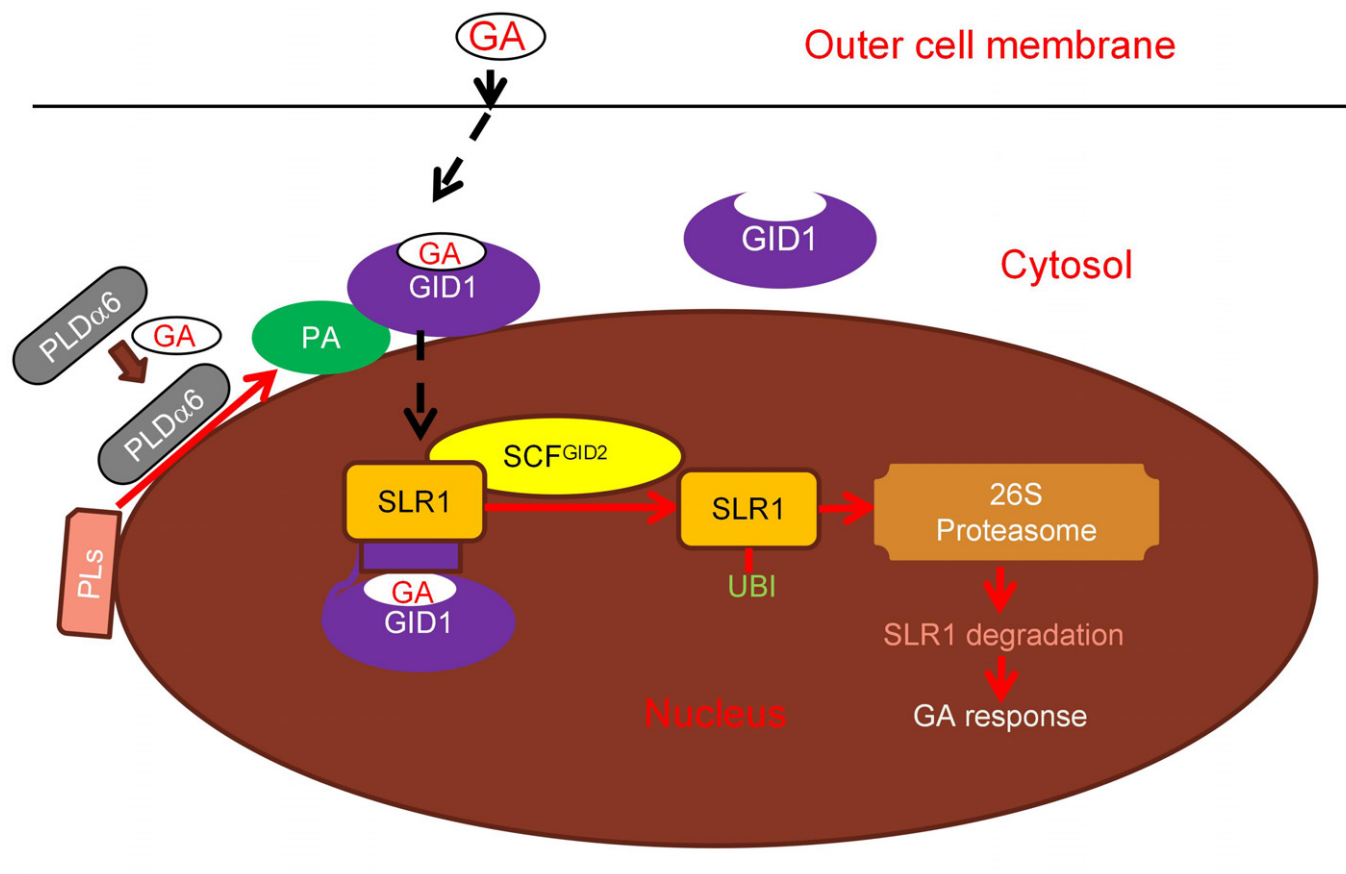


**Figure 8. Model of PLD $\alpha$ 6/PA and GID1 interaction and function in GA signaling.**

GA promotes PLD $\alpha$ 6 translocation from cytosol to the nucleus, resulting in an increase of PA in nuclear membranes. PA binds to GID1, tethers it to the membrane, and facilitates its nuclear translocation and the degradation of the suppressor SLR1, enhancing rice response to GA. PLs, phospholipids.

from cytosol to nuclei in response to GA, resulting in the production of more PA in nuclear envelope membranes. PA binds to GID1, resulting in the tethering of GID1 to nuclear membranes and facilitating the movement of GID1 from cytosol into the nucleus and interaction with the DELLA SLR1. The loss of PLD $\alpha$ 6 attenuated the degradation of SLR1, which is consistent with the current model that the GA-GID1-SLR1 interaction is required for the degradation of the suppressor SLR1. Taken together, present results indicate that the lipid mediator PA and PLD $\alpha$ 6 are new modulators in GA signaling, and they promote the nuclear localization of GID1 and enhance the GA suppressor DELLA degradation to enhance GA signaling and response. Further investigations are needed to establish the *in vivo* relevance of PA-GID1 interactions and its role in mediating nuclear localization.

## Materials and Methods

### Knockout mutant isolation and genetic complementation

A T-DNA insert mutant in *PLD $\alpha$ 6*, designated as *pld $\alpha$ 6*, was identified from the stock at Salk Institute Genomic Analysis Laboratory (<http://signal.salk.edu/>). A *PLD $\alpha$ 6* homozygous T-DNA insert

mutant was isolated by PCR using the primer *PLD $\alpha$ 6-1F/1R* and border primer *PLD $\alpha$ 6-2* (Appendix Table S1). A pair of *PLD $\alpha$ 6*-specific primer *PLD $\alpha$ 6-3F/3R* was used in RT-PCR to confirm the *PLD $\alpha$ 6* null mutant. To complement *pld $\alpha$ 6*, the native *PLD $\alpha$ 6* plus 2 kb upstream of the start codon of *PLD $\alpha$ 6* was amplified and cloned into the pU2301 vector (Zhou *et al*, 2016). The plasmid was transformed into *pld $\alpha$ 6* plants by agrobacterium-mediated transformation (Deng *et al*, 2019). The transformants were selected by hygromycin resistance and confirmed by PCR using the primer *PLD $\alpha$ 6-4F/4R*. The primers used are listed in Appendix Table S1.

### Plant growth and treatments

WT, *pld $\alpha$ 6*, and COM (*PLD $\alpha$ 6* complementation) plants were grown in 1/2 MS liquid media in growth chambers under 12-h light/12-h dark photoperiods ( $100 \mu\text{mol m}^{-2} \text{s}^{-1}$ ) at 28/23°C and 50% humidity. To screen for altered GA response, 3-day-old seedlings of WT and several PLD mutants (Appendix Table 2) were transferred to 0.5 MS liquid media with or without  $1 \mu\text{M}$  GA $_3$  and seedling growth was measured a week after the treatment. For further GA treatment experiments, one-week-old rice seedlings were treated with various concentrations (0, 0.1, 1, 10  $\mu\text{M}$ ) of GA $_3$  and growth phenotypes were measured at different time intervals. The control seedlings

were sprayed with the same volume of solution without GA<sub>3</sub> and shown as a mock.

### Subcellular localization of PLD $\alpha$ 6 and GID1

Rice *PLD $\alpha$ 6* and *GID1* cDNAs were cloned by PCR amplification from a rice leaf cDNA pool using the primers *PLD $\alpha$ 6-5F/5R* and *GID1-1F/1R* (Appendix Table S1). The PCR products were cloned into the pM999 that contains the p35S promoter and eGFP fusion at the C-terminus. The PCR product of *GID1* was used as the template to generate a series of site-directed mutants in *GID1*. *PLD $\alpha$ 6*, *GID1*, and *GID1* mutants in pM999 were transfected into rice protoplasts for protein expression and subcellular localization. In brief, rice protoplasts were isolated from 15-day-old seedling (ZH11 background), and the pM999-*PLD $\alpha$ 6*, pM999-*GID1*, and pM999-*GID1* mutant constructs were transfected to protoplasts by a polyethylene glycol (PEG)-mediated transformation. After 12- to 16-h incubation, GFP fluorescence was observed with a Lecia TCS SP2 confocal microscope. pM999-Ghd7 was transfected into protoplasts as a nuclear marker. GA<sub>3</sub> of various concentrations (0, 0.1, 1, 10  $\mu$ M) or 10  $\mu$ M IAA was added to protoplasts to test its effect on the subcellular distribution.

Transient expression in tobacco leaves was also used for examining the intracellular distribution of *PLD $\alpha$ 6* and *GID1*. *PLD $\alpha$ 6*-GFP, *GID1*-GFP, and *GID1* mutant-GFP constructs were introduced into *Agrobacterium tumefaciens* strain GV1301 by electroporation, and transformants were selected on LB plates containing 50 mg/ml kanamycin. Transformants were grown overnight in 5 ml liquid LB media and then centrifuged at 4,000 rpm for 10 min. The pellets were resuspended with 10 mM MgCl<sub>2</sub> plus 10  $\mu$ l 100 mM acetosyringone to OD<sub>600</sub> = 1.0 and used for infiltrating leaves on 4-week-old *Nicotiana benthamiana* plants. To facilitate the production of recombinant proteins, *agrobacteria* expressing the viral p19 protein that inhibits post-transcriptional gene silencing was co-infiltrated. The production of *PLD $\alpha$ 6*-GFP and *GID1*-GFP proteins was visualized 2–3 days after infiltration, and the fluorescence images were observed using a Lecia TCS SP2 confocal microscope. DAPI (4',6-diamidino-2-phenylindole) was used for nuclear staining. For hormone treatments, the infiltrated leaves were sprayed with GA<sub>3</sub> or IAA at indicated concentrations for subcellular localization.

The subcellular fractionation analysis was performed using rice protoplasts and tobacco leaves as described with some modifications (Shen *et al*, 2019); the above infiltrated tobacco leaves or protoplast infected were homogenized with a chilled buffer (25 mM Tris-HCl, pH 7.5, 100 mM NaCl, 10% glycerol, 1 mM EDTA, 1 mM EGTA, 1% NP40, and 0.5 mM PMSF) (Deng *et al*, 2019). The homogenate was filtrated through 300 mesh sieves, and the filtered product was centrifuged at 1,500 g for 5 min at 4°C to obtain the crude supernatant and nuclear (pellet) fractions. The resulting supernatants were centrifuged at 12,000 g for 5 min at 4°C to obtain soluble fraction. Equal amounts of proteins from different fractions including total, nuclear, and soluble fraction were separated by 8% (w/v) SDS-PAGE and then transferred onto a polyvinylidene difluoride (PVDF) membrane for immunoblotting. After that, the membrane was incubated with anti-GFP antibody (Sangon Biotech D110008) and then a secondary antibody conjugated with alkaline phosphatase (Sangon Biotech D110072) for 2-h incubation before color development using a chemiluminescence method.

### Expression and purification of His-tagged PLD $\alpha$ 6, GID1, and SLR1 protein

The cDNAs of *PLD $\alpha$ 6*, *GID1*, and *SLR1* were amplified with primers *PLD $\alpha$ 6-6F/6R*, *GID1-2F/2R*, and *SLR1-1F/1R* and then inserted into the pET28 vector. The deletion fragments *GID1*<sub>1-119</sub>, *GID1*<sub>1-138</sub>, *GID1*<sub>51-354</sub>, *GID1*<sub>120-354</sub>, and *GID1*<sub>139-354</sub> were amplified using the pairs of primers *GID1-2F/GID1-119R*, *GID1-2F/GID1-138R*, *GID1-511F/GID1-2R*, *GID1-120F/GID1-2R*, and *GID1-139F/GID1-2R* (Appendix Table S1). To generate the site-specific mutation of *GID1*, three full-length *GID1* cDNA was used as the template for PCR amplification with mutant primers *GID1-512F/R*, *GID1-52F/R*, *GID1-58F/R*, *GID1-79F/R*, *GID1-82F/R*, *Gid98-F/R*, *GID1-5152F/R*, *GID1-7982F/R*, and *GID1-2F/2R* (Appendix Table S1) to generate *GID1*<sub>R51A</sub>, *GID1*<sub>R52A</sub>, *GID1*<sub>R58A</sub>, *GID1*<sub>R79A</sub>, *GID1*<sub>R82A</sub>, *GID1*<sub>R98A</sub>, *GID1*<sub>R51AR52A</sub>, and *GID1*<sub>R79AR82A</sub>. All these *GID1* mutation products were inserted into the pET28 expression vector. The plasmids were transformed into the *Escherichia coli* strain BL21 (DE3) and cultured in LB media. Bacteria harboring the plasmids grown to OD<sub>600</sub>  $\approx$  0.4–0.6 were induced with 0.4 mM isopropyl 1-thio- $\beta$ -D-galactopyranoside (IPTG) for 4 h at 28°C. The expressed proteins were purified with 6xHis agarose beads (Novagen) according to the manufacturer's instruction, and the amount of protein was determined using the dye-binding protein assay kit (Bio-Rad).

### PLD $\alpha$ 6 activity assay

*PLD $\alpha$ 6* activity was assayed using the condition previously described (Hong *et al*, 2008). Briefly, the reaction contained a buffer (50 mM CaCl<sub>2</sub>, 100 mM MES, pH 6, 0.5 mM SDS) and 0.4 mM of lipid substrates (PC, PE, PG, or PS) which were dried under a stream of nitrogen and suspended in H<sub>2</sub>O by sonication. Different Ca<sup>2+</sup> concentrations from 0, 50 nM, 50  $\mu$ M, to 50 mM were tested with PC as substrate. After the addition of purified *PLD $\alpha$ 6*, the reaction was incubated for 30 min at 30°C and stopped by adding 1 ml of chloroform:methanol (1:2, v/v) and 0.2 ml of 1 M NaCl. The organic phase was dried under a stream of nitrogen and dissolved in 20  $\mu$ l of chloroform. The product was loaded onto silica gel plate (Merck, TLC silica gel 60) and separated by the developing solvent chloroform:ethanol:triethylamine:water (10:11.3:11.7: 2.7 v/v); TLC plate was exposed to iodine to visualize lipids. Lipid spots corresponding to that of the PA standard were scraped from the TLC plate. Five  $\mu$ l of 5.4  $\mu$ M 17:0 TAG was added to the sample as an internal standard, and the mixture was transmethylated in methanol containing 1% H<sub>2</sub>SO<sub>4</sub> and 0.05% butylated hydroxytoluene at 90°C for 1 h. One milliliter of hexane and 1 ml of water were added, and the upper phase was removed for GC analysis. The amount of PA was determined by comparing the amount of fatty acids in PA with that in the internal fatty acid standard. *PLD* activities toward PC, PE, PG, and PS were calculated based on the PA quantification from the TLC plate, using *PLD* produced PA = PA detected with *PLD $\alpha$ 6* – PA with empty vector in the presence of a specific phospholipid (Peters *et al*, 2010).

### Lipid–protein blotting and liposomal binding

The binding between protein and lipids on filters was performed as described (Stevenson *et al*, 1998; Cao *et al*, 2016) with some

modifications. Lipids (5  $\mu$ g) including PA, PC, PE, PG, and PS were spotted on a nitrocellulose filter, followed by incubation with purified His-tagged protein to the final concentration of 0.5 mg/ml in PBST (0.1% Tween 20) overnight at 4°C. The filter was then washed and incubated with anti-His antibody conjugated with alkaline phosphatase (Sigma). GID1 and SLR1 proteins that bound to lipids on filters were visualized by staining alkaline phosphatase activity.

Liposomal binding was performed as previously described with some modifications (Cao *et al*, 2016). Dioleoyl PC alone or mixed with dioleoyl PA (molar ratio 3:1) was dissolved in chloroform and dried under a stream of nitrogen. Lipids were rehydrated in a buffer (250 mM raffinose, 25 mM HEPES, pH 7.5, and 1 mM DTT) for 1 h at 42°C. Liposomes were produced using a liposome extruder (Avanti) to produce small unilamellar liposomes. Liposomes were diluted to 3.2 mM. For each assay, 320 nmol and 32 nmol of liposomes were incubated with GID1 and SLR1 proteins for 45 min at room temperature. A negative control used the binding mixture but without liposome added. Liposomes were pelleted at 14,000 g for 30 min, washed twice with the binding buffer, and pelleted again. Both liposome-bound proteins and proteins remaining in the supernatants were detected by immunoblotting with anti-poly His antibodies conjugated with alkaline phosphatase (1:10,000).

### Surface plasmon resonance analysis

Surface plasmon resonance analysis was performed using a Biacore 2000 system as described with some modifications (Guo *et al*, 2012b). Purified His-tagged GID1 (2  $\mu$ M) was immobilized on the Biacore Sensor Chip NTA via Ni<sup>2+</sup>-NTA chelation. For all experiments, running buffer (0.01 M HEPES, 0.15 M NaCl, 50  $\mu$ M EDTA, pH 7.4) containing 500  $\mu$ M NiCl<sub>2</sub> was injected to saturate the NTA with nickel. Di18:1-PA/di18:1-PC liposomes (200  $\mu$ M) were suspended in the running buffer and injected in sequence over the surface of the sensor chip. The liposomes containing dioleoyl PC, PG, or PS only were used for control. The sensorgrams of association and dissociation for each protein–liposome interaction were determined and plotted by SigmaPlot 10.0. Kinetic constants, including association rate constant ( $k_a$ ), an intermediate dissociation rate constant ( $k_d$ ), and the equilibrium binding affinity constant ( $K_D$ ), were analyzed using BIA evaluation software.

### qRT-PCR analysis of gene expression

To monitor the expression pattern of rice *PLD*s, seedling, leaf, leaf sheath, and root samples were collected from the 4-leaf stage rice (Dongjin). Stem and inflorescence samples were collected from the heading stage. For hormone treatments, 10  $\mu$ M GA<sub>3</sub>, KT, and NAA were sprayed on the leaves of 4-leaf stage rice seedlings, and 2 h later, leaves were collected for RNA extraction. To test the expression pattern of genes involved in GA signaling and metabolism, leaf tissues from 4-leaf stage WT and *pld $\alpha$ 6* were collected. Total RNA from rice tissues was extracted using a TransZol reagent according to the manufacturer's instruction (Transgen Biotech) and treated with DNaseI (Thermo). cDNA synthesis was performed with TIAN-script RT Kit (Transgen Biotech) from 5  $\mu$ g of DNA-free RNA and diluted to a final volume of 200  $\mu$ l. A total of 4  $\mu$ l of diluted cDNA was used for each quantitative RT-PCR (qRT-PCR) reaction. qRT-PCRs were prepared using SYBR Green Master Mix on a MyiQ

single-color real-time PCR detection system (Bio-Rad). *GAPDH* was used as a housekeeping gene to normalize the expression, and a 2<sup>- $\Delta$ CT</sup> method was used to calculate the transcript level of genes tested. The primer sequences used for qRT-PCR are listed in Appendix Table S1.

### Lipid analysis

Lipid profiling was carried out using the method described previously (Cao *et al*, 2016). Briefly, leaves from rice seedlings (4-leaf-old) were detached and immediately immersed in 4 ml of 75°C isopropanol (preheated) with 0.01% butylated hydroxytoluene (BHT) for 15 min, followed by the addition of 1.5 ml of chloroform and 0.5 ml of water. After shaking for 1–2 h, the solvent was transferred to a new clean tube. The leaves were re-extracted with 5 ml chloroform: methanol (2:1, v/v) six times with agitation for 45 min each, and the extracts were combined and then washed with 1 M KCl, followed by another wash with water. The solvent was evaporated by nitrogen, and the remaining tissue was oven-dried at 100°C and weighed. For each genotype and treatment, three leaf samples were extracted and analyzed separately. Lipid samples were introduced by continuous infusion into the ESI source on a triple quadrupole MS. Phospholipids and galactolipids were quantified by comparison of the peak for each lipid species to internal standards of the same class as described previously (Welti *et al*, 2002).

## Data availability

No data that require deposition in a public database.

**Expanded View** for this article is available online.

### Acknowledgements

This work was supported by National Natural Science Foundation of China (31701233, 31470762, and 31271514) and the Chinese National Key Basic Research Project (2012CB114200). This work was also supported by Department of Science and Technology of Guangdong Province Collaborative Innovation and Platform Construction Grant (No. 2017B090901069) and Special Fund for Scientific Innovation Strategy of Guangdong Province Construction of High-Level Academy of Agricultural Science.

### Author contributions

HC cloned expressed proteins, performed binding assays, activity assay, subcellular location, and phenotype analysis, and wrote the manuscript. RG made the complementary construct and rice transformation and field trail investigation and participated in article preparation. SY and YS analyzed the lipid data *in vivo*. WL and YZ isolated PLD mutants. QZ, XD, and PT participated in subcellular localization. SL, YH, and XW directed the project and article preparation.

### Conflict of interest

The authors declare that they have no conflict of interest.

## References

- Abreu FRM, Dedicova B, Vianello RP, Lanna AC, Oliveira JA, Vieira AF, Morais OP, Mendonça JA, Brondani C (2018) Overexpression of a phospholipase

- (OsPLD $\alpha$ 1) for drought tolerance in upland rice (*Oryza sativa* L). *Protoplasma* 255: 1751–1761
- Anthony RG, Henriques R, Helfer A, Mészáros T, Rios G, Testerink C, Munnik T, Deák M, Koncz C, Bögre L (2014) A protein kinase target of a PDK1 signalling pathway is involved in root hair growth in *Arabidopsis*. *EMBO J* 23: 572–581
- Awai K, Xu CC, Tamot B, Benning C (2006) A phosphatidic acid-binding protein of the chloroplast inner envelope membrane involved in lipid trafficking. *Proc Natl Acad Sci USA* 103: 10817–10822
- Cao H, Zhuo L, Su Y, Sun L, Wang X (2016) Non-specific phospholipase C1 affects silicon distribution and mechanical strength in stem nodes of rice. *Plant J* 86: 308–321
- Deng X, Yuan S, Cao H, Lam S, Shui G, Hong Y, Wang X (2019) Phosphatidylinositol-hydrolyzing phospholipase C4 modulates rice response to salt and drought. *Plant Cell Environ* 42: 536–548
- Gao H, Chu Y, Xue H (2013) Phosphatidic acid (PA) binds PP2AA1 to regulate PP2A activity and PIN1 polar localization. *Molecular Plant* 6: 1692–1702
- Guo L, Devaiah S, Narasimhan R, Pan X, Zhang Y, Zhang W, Wang X (2012a) Cytosolic glyceraldehyde-3-phosphate dehydrogenases interact with phospholipase D $\delta$  to transduce hydrogen peroxide signals in the *Arabidopsis* response to stress. *Plant Cell* 24: 2200–2212
- Guo L, Mishra G, Markham JE, Li M, Tawfall A, Welti R, Wang X (2012b) Connections between sphingosine kinase and phospholipase D in the abscisic acid signaling pathway in *Arabidopsis*. *J Biol Chem* 287: 8286–8296
- Hirano K, Asano K, Tsuji H, Kawamura M, Mori H, Kitano H, Ueguchi-Tanaka M, Matsuoka M (2010) Characterization of the molecular mechanism underlying gibberellin perception complex formation in rice. *Plant Cell* 22: 2680–2696
- Hong Y, Pan X, Welti R, Wang X (2008) Phospholipase D $\alpha$ 3 is involved in the hyperosmotic response in *Arabidopsis*. *Plant Cell* 20: 803–816
- Hong Y, Zhao J, Guo L, Kim S, Deng X, Wang G, Zhang G, Li M, Wang X (2016) Plant phospholipases D and C and their diverse functions in stress responses. *Prog Lipid Res* 62: 55–74
- Hu Y, Zhou L, Huang M, He X, Yang Y, Liu X, Li Y, Hou X, Hu Y, Zhou L et al (2018) Gibberellins play an essential role in late embryogenesis of *Arabidopsis*. *Nat Plants* 4: 289–298
- Huang S, Gao L, Blanchoin L, Staiger C (2006) Heterodimeric capping protein from *Arabidopsis* is regulated by phosphatidic acid. *Mol Biol Cell* 17: 1946–1958
- Huo C, Zhang B, Wang H, Meng F, Liu M, Gao Y, Zhan W, Deng Z, Sun D, Tang W (2016) Comparative study of early cold-regulated proteins by two dimensional difference gel electrophoresis reveals a key role for phospholipase D $\alpha$ 1 in mediating cold acclimation signaling pathway in rice. *Mol Cell Proteomics* 15: 1397–1411
- Li G, Lin F, Xue H (2007) Genome-wide analysis of the phospholipase D family in *Oryza sativa* and functional characterization of PLD $\beta$ 1 in seed germination. *Cell Res* 17: 881–894
- Li G, Xue H (2007) *Arabidopsis* pld $\zeta$ 2 regulates vesicle trafficking and is required for auxin response. *Plant Cell* 19: 281–295
- Li J, Henty-Ridilla J, Staiger B, Day B, Staiger C (2015) Capping protein integrates multiple MAMP signalling pathways to modulate actin dynamics during plant innate immunity. *Nat Commun* 6: 7206
- Li J, Pleskot R, Henty-Ridilla J, Blanchoin L, Potocký M, Staiger C (2012) Capping protein modulates the dynamic behavior of actin filaments in response to phosphatidic acid in *Arabidopsis*. *Plant Signal Behav* 24: 3742–3754
- McLoughlin F, Arisz S, Dekker H, Kramer G, de Koster C, Haring M, Munnik T, Testerink C (2013) Identification of novel candidate phosphatidic acid-binding proteins involved in the salt-stress response of *Arabidopsis thaliana* roots. *Biochem J* 450: 573–581
- Min MK, Kim SJ, Miao Y, Shin J, Jiang L, Hwang IH (2007) Overexpression of *Arabidopsis* AGD7 causes relocation of Golgi-localized proteins to the endoplasmic reticulum and inhibits protein trafficking in plant cells. *Plant Physiol* 143: 1601–1614
- Mishra G, Zhang W, Deng F, Zhao J, Wang X (2006) A bifurcating pathway directs abscisic acid effects on stomatal closure and opening in *Arabidopsis*. *Science* 312: 264–266
- Peters C, Li M, Narasimhan R, Roth M, Welti R, Wang X (2010) Nonspecific phospholipase C NPC4 promotes responses to abscisic acid and tolerance to hyperosmotic stress in *Arabidopsis*. *Plant Cell* 22: 2642–2659
- Qi J, Zhou G, Yang L, Erb M, Lu Y, Sun X, Cheng J, Lou Y (2011) The chloroplast-localized phospholipases D  $\alpha$ 4 and  $\alpha$ 5 regulate herbivore-induced direct and indirect defenses in rice. *Plant Physiol* 157: 1987–1999
- Sang Y, Zheng S, Li W, Huang B, Wang X (2001) Regulation of plant water loss by manipulating the expression of phospholipase D. *Plant J* 28: 135–144
- Shen P, Wang R, Jing W, Zhang W (2011) Rice phospholipase D is involved in salt tolerance by the mediation of H<sup>+</sup>-ATPase activity and transcription. *J Integr Plant Biol* 53: 289–299
- Shen Q, Zhan X, Yang P, Li J, Chen J, Tang B, Wang X, Hong Y (2019) Dual activities of plant cGMP-dependent protein kinase and its roles in gibberellin signaling and salt stress. *Plant Cell* 31(12): 3073–3091
- Stevenson J, Perera I, Boss W (1998) A phosphatidylinositol 4-kinase pleckstrin homology domain that binds phosphatidylinositol 4-monophosphate. *J Biol Chem* 273: 22761
- Sun TP (2010) Gibberellin-GID1-DELLA: a pivotal regulatory module for plant growth and development. *Plant Physiol* 154: 567–570
- Testerink C, Munnik T (2005) Phosphatidic acid: a multifunctional stress signaling lipid in plants. *Trends Plant Sci* 10: 368–375
- Ueguchi-Tanaka M, Ashikari M, Nakajima M, Itoh H, Katoh E, Kobayashi M, Chow T-Y, Hsing Y-ie C, Kitano H, Yamaguchi I et al (2005) GIBBERELLIN INSENSITIVE DWARF1 encodes a soluble receptor for gibberellin. *Nature* 437: 693–698
- Ueguchi-Tanaka M, Nakajima M, Katoh E, Ohmiya H, Asano K, Saji S, Hongyu X, Ashikari M, Kitano H, Yamaguchi I et al (2007) Molecular interactions of a soluble gibberellin receptor, GID1, with a rice DELLA protein, SLR1, and gibberellin. *Plant Cell* 19: 2140–2155
- Wang X (2004) Lipid signaling. *Curr Opin Plant Biol* 7: 329–336
- Wang X, Devaiah SP, Zhang W, Welti R (2006) Signaling functions of phosphatidic acid. *Prog Lipid Res* 45: 250–278
- Welti R, Li W, Li M, Sang Y, Biesiada H, Zhou H-E, Rajashekar CB, Williams TD, Wang X (2002) Profiling membrane lipids in plant stress responses: role of phospholipase D $\alpha$  in freezing-induced lipid changes in *Arabidopsis*. *J Biol Chem* 277: 31994–32002
- Xue W, Xing Y, Weng X, Zhao Yu, Tang W, Wang L, Zhou H, Yu S, Xu C, Li X et al (2009) Natural variation in Ghd7 is an important regulator of heading date and yield potential in rice. *Nat Genet* 40: 761–767
- Yamaguchi T, Kuroda M, Yamakawa H, Ashizawa T, Hirayae K, Kurimoto L, Shinya T, Shibuya N (2009) Suppression of a phospholipase D gene, OsPLD $\beta$ 1, activates defense responses and increases disease resistance in rice. *Plant Physiol* 150: 308–319
- Yao H, Wang G, Guo L, Wang X (2013) Phosphatidic acid interacts with a MYB transcription factor and regulates its nuclear localization and function in *Arabidopsis*. *Plant Cell* 25: 5030–5042
- Yao H, Xue H (2018) Phosphatidic acid (PA) plays key roles regulating plant development and stress responses. *J Integr Plant Biol* 60: 851–863

- Yu L, Nie J, Cao C, Jin Y, Yan M, Wang F, Liu J, Xiao Y, Liang Y, Zhang W (2010) Phosphatidic acid mediates salt stress response by regulation of MPK6 in *Arabidopsis thaliana*. *New Phytol* 188: 762–773
- Zhang Q, Lin F, Mao T, Nie J, Yan M, Yuan M, Zhang W (2012) Phosphatidic acid regulates microtubule organization by interacting with MAP65-1 in response to salt stress in *Arabidopsis*. *Plant Cell* 24: 4555–4576
- Zhang W, Qin C, Zhao J, Wang X (2004) Phospholipase D $\alpha$ 1-derived phosphatidic acid interacts with ABI1 phosphatase 2C and regulates abscisic acid signaling. *Proc Natl Acad Sci USA* 101: 9508–9513
- Zhang Y, Zhu H, Zhan Q, Li M, Yan M, Wang R, Li L, Ruth W, Zhan W, Wang X (2009) Phospholipase dalpha1 and phosphatidic acid regulate NADPH oxidase activity and production of reactive oxygen species in ABA-mediated stomatal closure in *Arabidopsis*. *Plant Cell* 21: 2357–2377
- Zhou W, Wang X, Zhou D, Ouyang Y, Yao J (2016) Overexpression of the 16-kDa  $\alpha$ -amylase/trypsin inhibitor RAG2 improves grain yield and quality of rice. *Plant Biotechnol J* 15: 568–580